

RESEARCH ARTICLE | OCTOBER 09 2024

System size effects on the free energy landscapes from molecular dynamics of phase-separating bilayers

Ashlin J. Poruthoor ; Jack J. Stallone ; Megan Miaro ; Akshara Sharma ; Alan Grossfield  



J. Chem. Phys. 161, 145101 (2024)

<https://doi.org/10.1063/5.0225753>



AIP Advances

Why Publish With Us?

-  **21DAYS**
average time to 1st decision
-  **OVER 4 MILLION**
views in the last year
-  **INCLUSIVE**
scope

[Learn More](#)



System size effects on the free energy landscapes from molecular dynamics of phase-separating bilayers

Cite as: J. Chem. Phys. 161, 145101 (2024); doi: 10.1063/5.0225753

Submitted: 26 June 2024 • Accepted: 24 September 2024 •

Published Online: 9 October 2024



View Online



Export Citation



CrossMark

Ashlin J. Poruthoor,  Jack J. Stallone,  Megan Miaro,  Akshara Sharma,  and Alan Crossfield^{a)} 

AFFILIATIONS

Department of Biochemistry and Biophysics, University of Rochester Medical Center, Rochester, New York 14642, USA

^{a)} Author to whom correspondence should be addressed: alan_grossfield@urmc.rochester.edu

ABSTRACT

The “lipid raft” hypothesis proposes that cell membranes contain distinct domains of varying lipid compositions, where “rafts” of ordered lipids and cholesterol coexist with disordered lipid regions. Experimental and theoretical phase diagrams of model membranes have revealed multiple coexisting phases. Molecular dynamics (MD) simulations can also capture spontaneous phase separation of bilayers. However, these methods merely determine the sign of the free energy change upon phase separation—whether or not it is favorable—but not the amplitude. Recently, we developed a workflow to compute the free energy of phase separation from MD simulations using the weighted ensemble method. However, while theoretical treatments generally focus on infinite systems and experimental measurements on mesoscopic to macroscopic systems, MD simulations are comparatively small. Therefore, if we are to put the results of these calculations into the appropriate context, we need to understand the effects the finite size of the simulation has on the computed free energy landscapes. In this study, we investigate this phenomenon by computing free energy profiles for a model phase-separating system as a function of system size, ranging from 324 to 10 110 lipids. The results suggest that, within the limits of statistical uncertainty, bulk-like behavior emerges once the systems contain roughly 4000 lipids.

Published under an exclusive license by AIP Publishing. <https://doi.org/10.1063/5.0225753>

I. INTRODUCTION

Cell membranes are often compositionally heterogeneous, spontaneously forming domains exhibiting collective behavior and preferential interactions.^{1–5} The formation of such functional domains has been attributed to liquid-liquid phase separation, which can be recapitulated in simple model membranes.^{6–10} However, the biological importance of phase separation in membranes and the size, lifetime, biochemical makeup, and functional importance of the resulting domains have been debated for many years.^{11–14} Recent studies have proposed an adaptable fluid mosaic model for biological membranes, spatially tuned to reside close to a critical point so that the phase separation can be used for functional roles.^{15,16}

Due to their high spatial and temporal resolution, molecular dynamics (MD) simulations have been used extensively to study phase separation in lipid mixtures and augment the experimental results.^{17–23} Although all-atom MD simulation studies of lipid phase separation have been reported,^{24–30} previous studies have

predominantly used coarse-grained models to minimize the computational expense. This was necessary because capturing phase separation requires a relatively large simulation. While spontaneous separation may occur on time scales accessible to MD, estimating the thermodynamic favorability of the process would require a significant number of reversible transitions, which is prohibitively slow. To circumvent this limitation, we developed FLOPSS,³¹ a workflow built on the weighted ensemble method^{32–34} to compute the membrane phase separation thermodynamics from MD by enhancing the sampling³⁵ along a novel clustering-based collective variable.

Systematic errors can arise while estimating thermodynamic quantities from simulations due to the finite size of the simulation box.³⁶ Previous studies have explored the system-size effect on computing transport properties such as translational diffusion coefficients and viscosities,^{37–40} on free energies of solvation,⁴¹ and nucleation⁴² from MD simulations. Such finite-size effects are also well-documented for lipid bilayer systems.^{43–48} Therefore, it is

necessary to know the extent and meaning of fluctuations and correlated motions within the system and how they affect the computed bulk properties.⁴⁹ Ideally, a simulation would be large enough to approach the thermodynamic limit, where the bulk-like behavior is independent of the extent of the system. Recently, a systematic study of finite-size effects on the domain formation in a ternary lipid bilayer using standard MD simulation with systems ranging from 240 to 5406 lipids suggested a lower limit for macroscale domain formation and estimated that the thermodynamic limit would require systems of 10 000 lipids or more.⁵⁰ A similar conclusion was reached in a study applying Monte Carlo sampling to a lattice model of lipid mixtures.^{51,52}

Inspired by these studies, we use molecular dynamics simulations to investigate finite-size effects on the free energy landscapes of a phase-separating ternary lipid bilayer. The ternary lipid bilayer that we investigate consists of dipalmitoylphosphatidylcholine (DPPC), dilinoleyl-phosphatidylcholine (DIPC), and cholesterol (CHOL), at a molar ratio of 0.42:0.28:0.3. We use the FLOPSS workflow to estimate the free energy landscapes of forming distinct domains in this system as a function of system size ranging from 324 lipids to 10 110 lipids while keeping the lipid composition and hydration the same. We track the evolution of these free energy curves and $\Delta\Delta G_{\text{sep}}$ with system size and show that most quantities appear to become bulk-like once the systems have roughly 4000 lipids.

II. METHODS

As reported previously,³¹ FLOPSS is a workflow to compute the free energy landscapes of phase-separating systems which, we tested on multiple ternary lipid bilayer systems simulated at varying temperatures. The workflow starts with building the bilayer replicates, followed by running standard MD simulations. These standard simulations are then used to collect seed configurations for weighted ensemble MD simulations to enhance the sampling of mixing and demixing the bilayer. In our original FLOPSS study, we showed that the choice of progress coordinate is not trivial and can lead to misleading conclusions due to poor convergence. We reported that a progress coordinate based on the clustering of lipids can be an excellent choice. In this study, we applied the same protocol to DPPC-DIPC-CHOL systems of varying sizes, using the coordinate designated as FLC_{opt} in our original work.

A. System construction and standard MD simulation

Using the MARTINI-MAKER module from CHARMM-GUI,⁵³ we built DPPC-DIPC-CHOL systems in a molar ratio of 0.42:0.28:0.3, with varying sizes ranging from 324 to 10 110 lipids; see Table I for a complete listing of systems. For each system size, we built four independent replicates. MARTINI 2.x particle parameters and force field parameters^{54,55} were used, along with MARTINI polarizable water.⁵⁶ An approximate 1:30 lipid:real water ratio was maintained in all systems. Following the CHARMM-GUI Martini Maker default protocol, each system was minimized and equilibrated in steps using the GROMACS 2020.3 package.⁵⁷ However, to prevent the excessive membrane undulations that were previously reported to be associated with large membrane systems,^{58–60} we applied a flat-bottomed restraint potential⁶¹ with a well radius of 2.3125 nm and force constant $k = 1000 \text{ KJ mol}^{-1} \text{ nm}^{-2}$ to the PO4 beads of phosphatidylcholine lipids.

All production simulations were performed using GROMACS 2020.3. Unless otherwise mentioned, we have adopted previously reported MARTINI simulation parameters.⁶² For van der Waals interaction, a potential-shift van der Waal's modifier was used with a 1.1 nm cutoff. For electrostatics, we used the reaction field method⁶³ with a 1.1 nm Coloumb cutoff and a dielectric constant of 2.5. The verlet cutoff scheme⁶⁴ with a neighbor list update frequency of 20 time steps was used for neighbor searching. Extended-ensemble Parrinello–Rahman pressure coupling⁶⁵ was used with a 12 ps time constant, a compressibility of $3 \times 10^{-4} \text{ bars}^{-1}$, and 1 bar reference pressure. Velocity rescaling⁶⁶ with a 1 ps time constant was used for temperature coupling. For better accuracy and energy conservation, we used the LINCSolver constraint coupling matrix⁶⁷ with 8th order expansion and a short 20 fs time step, respectively.⁶⁸ These choices were based on previous reports of artifacts due to inaccurate constraints in MARTINI coarse-grained bilayer simulations. For all replicates, an initial 100 ns run at 400 K in the NPT ensemble was followed by two independently forked 4 μs standard MD production runs, at 323 and 423 K, respectively. The low-temperature runs were used to sample the phase separated state and transitional values, while the 423 K remained mixed. The short high-temperature run at the beginning was intended to ensure random mixing of lipids at the starting state since some demixing occurred during the equilibration process.

TABLE I. Details of lipid composition, solvation, and dimensions of the different systems under study. Average box dimensions are calculated after 4 μs standard MD production run at 323 K (supplementary material, Table S1).

Total number of lipids	No. of DPPC (0.42)	No. of DIPC (0.28)	No. of cholesterol (0.3)	Total CG wate	Average box dimensions (x × y × z) (Å)
324	138	90	96	2430	117.8 × 115.8 × 66.7
648	276	180	192	4860	159.2 × 159.2 × 66.9
972	414	270	288	7290	194.9 × 192.4 × 66.2
1944	828	540	576	14 580	265.1 × 265.5 × 69.1
3888	1656	1080	1152	29 160	370.9 × 370.4 × 68.8
7776	3312	2160	2304	58 320	513.9 × 513.4 × 71.3
10 110	4306	2808	2996	75 825	582.7 × 583.3 × 72.2

B. Choice of progress coordinate

A progress coordinate or collective variable is intended to represent the complex multidimensional dynamics of the system in a single dimension that is easy to track and interpret. Therefore, for the same system, a progress coordinate can vary depending on the question one is addressing. Frequently, progress coordinates are used to track the progress of the transition of interest in a system, which in our case is the transition of the bilayer from a mixed state to a separated state and vice versa. Progress coordinates are also central to the application of many enhanced sampling techniques, including the weighted ensemble method at the core of the FLOPSS workflow.^{34,69} Previously, we have reported that progress coordinates that correlate with phase separation in bilayers often do not enhance the sampling in WE simulations. We identified one effective choice, the Fraction of Lipids in Clusters (FLCs), defined as

$$\text{FLC} = \frac{\sum_i^N \text{No. of Lipid } X_i \text{ in Lipid } X_i \text{ Clusters}}{\text{Total No. of Lipids}}, \quad (1)$$

where subscript i denotes the individual lipid species in a bilayer consisting of N total lipid species. Since we have a ternary DPPC-DIPC-CHOL system, $N = 3$. FLC can range from 0 to 1, where $\text{FLC} = 1$ indicates a separated state where all lipids are part of some cluster. This clustering is performed using the Density-Based Spatial Clustering of Applications with Noise (DBSCAN) algorithm^{70,71} as implemented in scikit-learn.⁷² We pre-compute all lipid-lipid distances two-dimensionally, treating the two leaflets independently.

DBSCAN takes two parameters: the distance within which two lipids are considered neighbors and the minimum number of neighbors needed to form a cluster. In our previous work, we used two different sets of clustering parameters, but here we use the values we previously termed FLC_{opt} in our previous work, as these parameters do a better job of distinguishing mixed and separated states. The optimized set of values for the DPPC-DIPC-CHOL system were (26.5 Å, 24 neighbors), (31.5 Å, 26 neighbors), and (32.5 Å, 23 neighbors) for DPPC, DIPC and cholesterol, respectively.

C. Weighted ensemble simulation

Each iteration of the weighted ensemble (WE) algorithm contains two components. In the first, a number of “walkers” (conventional MD simulations) are propagated starting from each bin on the progress coordinate. In the second component, the progress coordinate is updated based on the state of the system at the end of each walker’s trajectory, and based on that, the walker is assigned to a bin. The target number of walkers per bin is maintained by merging or splitting walkers while conserving the statistical weight in each bin. More details on the theory and implementation of the weighted ensemble method can be found in recent reviews.^{34,73}

We ran two replicates of weighted ensemble simulations for each system size. We seeded each replicate by picking evenly spaced frames from the last microsecond of each of the conventional MD simulations. We used structures from both the 323 and 423 K simulations to ensure that the weighted ensemble simulations initially sampled both well-mixed and demixed states to speed equilibration and convergence of the WE simulations.

To propagate the WE simulations, we used WESTPA2 v2022.06⁷⁴ and followed the previously established protocols.^{31,73,75} A Minimal Adaptive Binning (MAB) scheme⁷⁶ was employed to divide the progress coordinate space into 30 dynamic bins. We set the target number of “walkers” per bin to 4. To speed up the convergence of WE simulations, the WE Equilibrium Dynamics (WEED) reweighting protocol^{77,78} was used with a reweighting window of ten iterations. It is not statistically correct to average values across multiple reweighting windows, so unless otherwise noted, the average values reported here are from the last ten iterations of the WE simulations. GROMACS 2020.3 was used to propagate the MD part of each iteration using the same settings detailed earlier.

For all the system sizes except 7778 and 10 110 lipids, each replicate completed WE 1000 iterations. The system with 7778 and 10 110 lipids completed 600 and 500 iterations, respectively, as the computational cost was significantly higher. However, for the systems that ran 1000 iterations, we saw that the results did not change significantly after the first 500 iterations.

All simulations were run using the BlueHive computing cluster in the Center for Integrated Research and Computing facility at the University of Rochester. Intel Xeon E5-2695, Gold 6130, 6140, and 6330 processors with Tesla K20Xm, K80, V100, and A100 GPUs were used to propagate the dynamics.

Simulation data were processed and analyzed with the LOOS software package.⁷⁹ The data from each WE replicate were combined using the w_multi_west tool in WESTPA2. Subsequently, WESTPA2 tools such as w_pdist and $plothist$ were used to construct the free energy landscapes, $\Delta G(\text{FLC})$. The data generated from WE simulations were projected onto other auxiliary variables to derive further insights using w_crawl and LOOS tools.

Once the free energy landscapes were constructed for each system, we calculated the average FLC, $\langle \text{FLC} \rangle$ as given below:

$$\langle \text{FLC} \rangle = \frac{\sum (\text{FLC} \rho(\text{FLC}))}{\sum \rho(\text{FLC})}, \quad (2)$$

where $\rho(\text{FLC})$ is the probability of finding the system at a particular FLC value as obtained from WE. Similarly, we can estimate the variance and standard deviation $\sigma(\text{FLC})$ by using the analogous formula for $\langle \text{FLC}^2 \rangle$. We also quantified the fluctuations in free energy curves by computing the variance $\Delta G(\text{FLC})$ over a range of FLC values. To compute the free energy difference between the mixed and phase-separated states of the system, $\Delta \Delta G_{\text{sep}}$, we identified the maximum value of ΔG within the range $\langle \text{FLC} \rangle \pm \sigma(\text{FLC})$ and considered that to be the barrier between the two states. To distinguish genuine barriers from statistical noise, we only considered the maximum to be a barrier if it was greater than $2\sigma(\Delta G)$.

III. RESULTS

A. Finite size effects from standard MD

Figure 1 shows the evolution of the FLC as a function of time from standard MD simulations that ran at 323 and 423 K, with four independent replicates simulated at each temperature. For all system sizes, the FLC values remain very low at 423 K, indicating that the lipids are well-mixed. By contrast, at 323 K, the FLC values increase rapidly over the first 100 ns of each trajectory before equilibrating

and remaining stable for the remainder of the trajectory, suggesting highly non-ideal mixing and possibly phase separation.

The average FLC values do not appear to vary significantly with system size at either temperature; this is visible in Fig. 1 and shown quantitatively in [supplementary material](#), Table S2. However, the fluctuations drop significantly as the system size increases, indicating qualitatively different behavior with different-sized systems. If we track the contribution of individual species to FLC, we see a similar trend, as shown in [supplementary material](#), Fig. S1.

To better understand the nature of the structural differences with system size, we tracked the size of the clusters formed by individual lipid species. Figure 2 shows the average size of lipid clusters as a function of system size as computed from the standard MD simulations. As expected, large clusters are not observed at the higher temperature. However, at 323 K, the mean cluster size increases with system size for the smallest systems. However, the average cluster size plateaus, within the limits of the statistical uncertainties, once there are roughly 2000 lipids in the system. This strongly suggests that smaller periodic boxes suppress the formation of larger aggregates.

B. Finite size effects on free energy landscapes from weighted ensemble molecular dynamics

Figure 3 shows the free energy curves obtained from WE MD runs, averaging over the last ten WE iterations. For the smaller systems, the free energy surfaces are flat and noisy. However, for larger systems than 3888 lipids, the free energy curves are smoother, with well-defined basins at relatively low FLC and high FLC values. This implies that the system can be found in a relatively mixed state (where fewer lipids are part of clusters) as well as a demixed state (where more lipids are part of clusters); based on previous analysis, the construction of the progress coordinate, and visual inspection, we interpret the high-FLC basin as the phase-separated one, while the lower-FLC basin is a single-phase but non-ideally mixed state.

For the smaller systems, virtually the entire range $0.2 < \text{FLC} < 0.8$ is thermodynamically accessible. However, for systems with 3888 lipids and larger, the width of the wells narrows, and the free energy increases more rapidly at the edges. For the two largest systems, the free energy curves are very similar.

One key question is whether the system size affects the morphology of the membrane; Fig. 2 showed this to be the case using the conventional MD simulations, but WE should allow a more complete exploration of the free energy landscape. Figure 4 shows the distribution of DPPC cluster sizes for all system sizes simulated. Except for the smallest 324-lipid system, the primary peak in the distribution is around 50–60 lipids in a cluster. However, the distribution is far from Gaussian, with a significant tail at large cluster sizes. Moreover, all of the distributions have a secondary large-cluster peak, but the location of this peak varies non-monotonically with system size. It is not clear whether this results from statistical noise due to poor convergence as large clusters slowly coalesce or if this is a genuine feature of the system.

C. Finite size effects on $\Delta\Delta G_{\text{sep}}$ estimation

The free energy difference between the mixed and the demixed states of the system, $\Delta\Delta G_{\text{sep}}$, can be obtained by defining an FLC

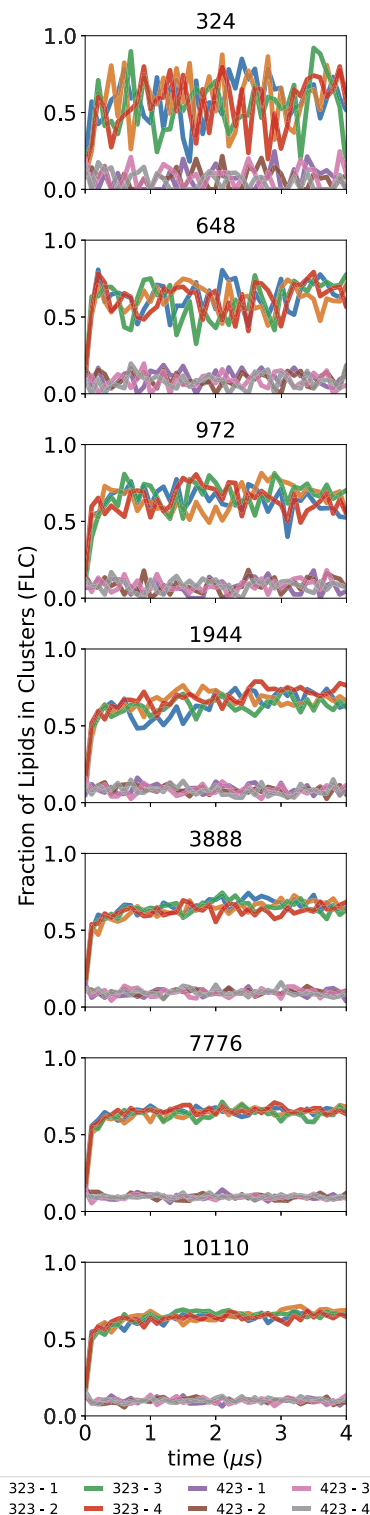


FIG. 1. Evolution of FLC of the system over 4 μs at 323 and 423 K. Line colors correspond to independent replicates simulated at different temperatures.

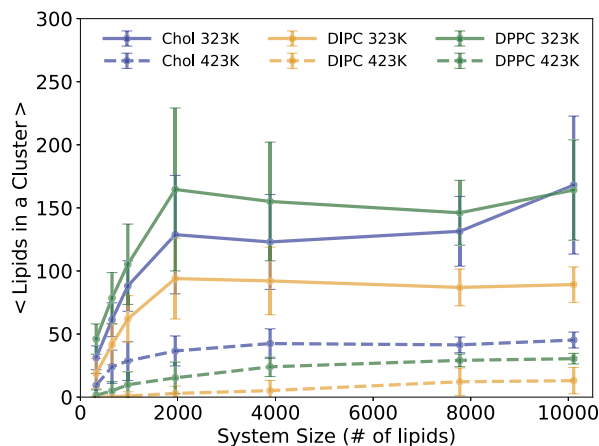


FIG. 2. Average size of lipid clusters as a function of system size. Dashed lines represent the simulations at 423 K, while solid lines show the data from the simulations at 323 K. The error bars are the standard error computed treating each replica as a single measurement.

cutoff that distinguishes one state from another and using the weights from the WE simulations to compute their relative probabilities,

$$\Delta\Delta G_{\text{sep}} = -k_B T \ln \frac{P_{\text{demixed}}}{P_{\text{mixed}}}. \quad (3)$$

The challenge, therefore, is to identify an appropriate cutoff in an unbiased manner. With a smooth two-well free energy curve, the choice is obvious: the local maximum of the free energy is the best choice. However, because the present simulations were run close to the transition temperature, where the barrier must go to zero because there are no longer two coexisting states, the statistical noise in the free energy curves is comparable to the barrier height. As a result, it was necessary to use a more robust procedure. As discussed in the Methods section, we compute the average and standard deviation of FLC from the ΔG curve and search for the highest local maximum within one standard deviation of the average. To distinguish noise from a genuine barrier, we only consider maxima whose values are greater than $2\sigma(\text{FLC})$. The free energy curves are computed by combining the data from two independent replicates; curves computed separately from the individual WE runs are shown in Fig. S9.

Figure 3 shows that, for the smaller systems, the free energy surfaces are relatively flat and noisy and do not resemble double-well free energy curves. Although we can apply the above-mentioned algorithm to calculate a $\Delta\Delta G_{\text{sep}}$ for them, in reality we would argue that phase separation does not occur. For the three largest systems (3888, 7776, and 10 110 lipids), the free energy curves do show a clear double-well shape; for the latter two, the location of the average and the walls are consistent, and our algorithm identifies similar FLC cutoffs.

The resulting $\Delta\Delta G_{\text{sep}}$ values are shown in Fig. 5. The estimated free energy changes are sensitive to the system size, fluctuating non-monotonically for the smaller systems; this is largely an artifact of the flat landscapes, making a separation into two states somewhat arbitrary. However, for the three largest systems, $\Delta\Delta G_{\text{sep}}$ is

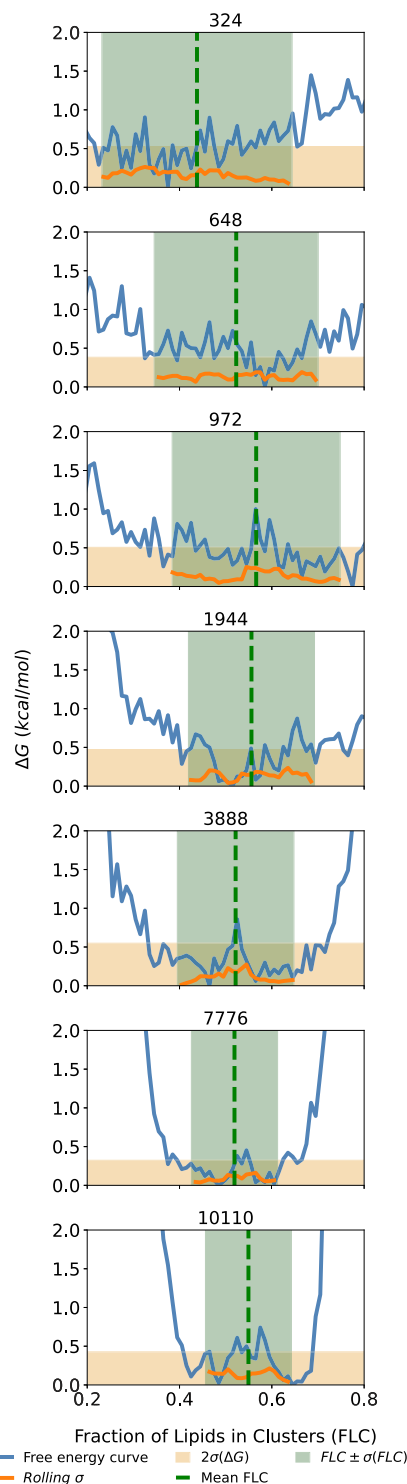


FIG. 3. Free energy landscapes for system sizes varying from 324 to 10 110 lipids (blue curves). For each system size, the vertically dotted dark green line indicates the average FLC, $\langle \text{FLC} \rangle$, the vertical light green slab indicates $\langle \text{FLC} \rangle \pm \sigma(\text{FLC})$, the orange line indicates the running standard deviation, and the horizontal light orange slab corresponds to $2\sigma(\Delta G)$ within the light green slab.

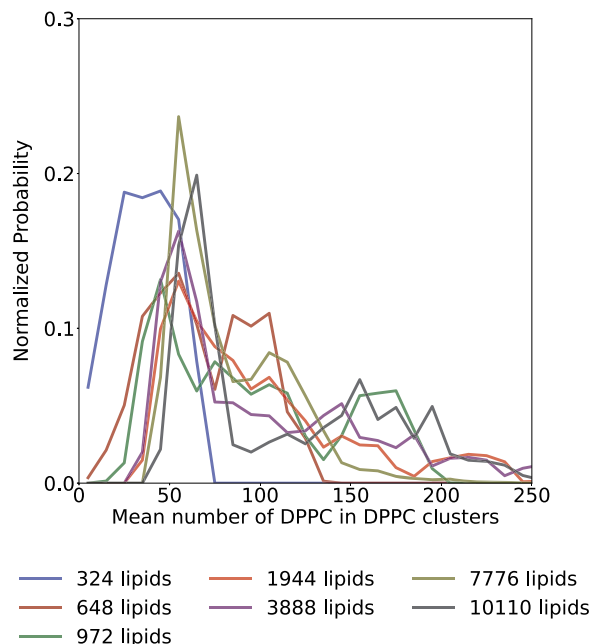


FIG. 4. Probability distribution for DPPC cluster sizes for all system sizes.

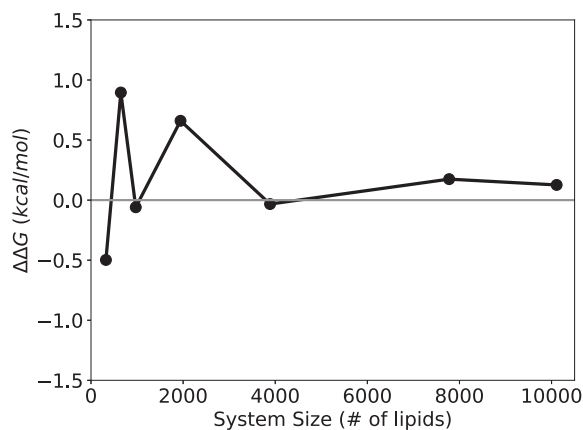


FIG. 5. Computed $\Delta\Delta G_{\text{sep}}$ for systems ranging from 324 lipids to 10 110 lipids.

consistent to within ≈ 0.1 kcal/mol. Consistent with our previous work,³¹ the values are slightly positive, indicating that the melting temperature for phase separation is roughly 323 K. This information would not be accessible from conventional simulations alone.

IV. DISCUSSION

Molecular dynamics simulations of lipid bilayers face a fundamental challenge in that they attempt to represent an infinite (or at least macroscopic) system with a finite number of molecules replicated via periodic boundary conditions. In a sense, we go into the calculations knowing that periodic boundaries are “wrong,” and

while they are clearly the least wrong choice, it is still crucial to understand how the finite size of the system affects the results.

This challenge is particularly acute when studying phase separation in lipid bilayers. The formation of domains is intrinsically a macroscopic or at least mesoscopic phenomenon, while atomistic simulations (even with coarse-grained potentials) are necessarily microscopic. Theoretical approaches generally assume an infinite system, or at least one large enough that the size of the system does not affect the results and tend to break down for smaller systems. Therefore, when attempting to compare simulations to experiments or theory, it is important to understand potential finite-size artifacts present in the simulations.

In this work, we leverage our recently developed technology for computing the free energy landscape of lipid phase separation³¹ to directly measure these finite-size effects. We conclude that small systems are unable to separate at all but rather undergo a wide range of fluctuations, as indicated by the wide, flat free energy curves. A barrier between the two states begins to emerge with the ≈ 2000 -lipid systems, and the two largest systems (≈ 8000 and $10\,000$ lipids, respectively) have free energy curves that are consistent within statistical error, while the $\Delta\Delta G_{\text{sep}}$ is consistent once the systems reach about 4000 lipids.

Figures S7 and S8 show representative snapshots of the systems at different values of FLC. We see that the larger systems do not form neat round domains at values of FLC corresponding to the phase-separated minimum of their respective free energy curves, around $\text{FLC} = 0.7$. Rather, there are large regions containing mostly DPPC and cholesterol, while DIPC-enriched regions are messier and less well-defined. Figure S8 shows that $\text{FLC} = 0.9$ corresponds to more “pure” separation, but the free energies are very high at this point for all but the smallest systems.

Previous studies have investigated finite-size effects in the simulation of lipid phase separation, although the present work is, to our knowledge, the first to use the free energy landscape as a read-out. For example, Pantelopulos *et al.*⁵⁰ performed coarse-grained simulations of a lipid composition similar to the one in this paper and tracked the number of order parameters as a function of system size. Although their largest simulation had roughly 5400 lipids, they extrapolated their systems’ behavior to estimate that bulk behavior would be observed for systems with 10 000 lipids. A previous lattice model simulation of two-component bilayer phase separation also concluded that 10 000 lipid systems were sufficiently large to eliminate finite-size effects.⁵¹

The free energy change upon phase separation, $\Delta\Delta G_{\text{sep}}$, is an extensive quantity and so should scale linearly with the system size. However, once the simulations are sufficiently large, all intensive quantities should become independent of system size. These include the ability to form coexisting phases and the transition temperature T_m , where coexisting phases melt into a single phase. Moreover, the composition of coexisting phases will also become independent of system size in the thermodynamic limit; in our data, this will show up as constant locations for the minima of the free energy curves. Unfortunately, because our simulations were run very close to T_m , the linear trend in $\Delta\Delta G_{\text{sep}}$ is not readily visible.

One additional challenge in interpreting this work is the potential for confusion due to an imperfect progress coordinate. Our previous work established that FLC produces results that make sense across a range of system compositions and temperatures, while other

intuitive coordinates, particularly those related to local enrichment of the density of individual lipid species, do not.³¹ That said, there is no guarantee that FLC perfectly correlates with the phase transition since it is sensitive to both the presence of multiple phases and to changes in the composition of those phases; this is why in previous work we saw shifts in the curves toward lower FLC with increasing temperature.³¹ We are currently pursuing other potential coordinates that may more directly correlate with the formation of distinct phases.

V. CONCLUSIONS

Whenever one tries to draw conclusions from simulations of phase separation (or similar bulk phenomena), one natural question to ask is whether the system is big enough to accurately represent the phenomenon in question. The present work uses the free energy landscape as a readout for the phase separation of a ternary lipid bilayer, measuring its dependence on the size of the simulation. We see that for very small systems, phase separation is entirely suppressed, but once the system approaches 10^4 lipids, more bulk-like behavior is observed. The present work has two limitations. First, using a ternary system means we do not know if the minimum bulk system size will change with the addition of more components, including other lipid species, transmembrane or peripheral proteins, etc. Second, it would be ideal to have system sizes far larger than our estimated threshold for the thermodynamic limit. However, the computational cost of such simulations is currently prohibitively high. As an alternative, we plan to perform analogous calculations using simpler lattice models, which should make calculations across 3–4 orders of magnitude in system size tractable.

SUPPLEMENTARY MATERIAL

See the [supplementary material](#) for simulation details. It contains further standard MD analysis details, including (1) mean and variance of FLC, (2) evolution of individual species contribution to FLC, (3) species-wise cluster count analysis, and (4) cluster size. The [supplementary material](#) also contains further weighted ensemble analysis such as individual species contribution to free energy landscapes and species-wise cluster size details. We also include snapshots of systems at representative levels of FLC in order to provide more intuition as to the meaning of phase separation in these systems.

ACKNOWLEDGMENTS

The authors acknowledge the Center for Integrated Research Computing (CIRC) at the University of Rochester for providing computational resources and technical support. A.J.P. acknowledges the Leon Miller Fellowship from the University of Rochester Medical Center. This work was supported by grant R21GM138970 (to AG) from the National Institutes of Health.

AUTHOR DECLARATIONS

Conflict of Interest

The authors have no conflicts to disclose.

Author Contributions

A.J.P. and A.G. designed the project. A.J.P., J.J.S., M.M., and A.S. performed the research. A.J.P. and A.G. wrote the paper.

Ashlin James Poruthoor: Conceptualization (equal); Investigation (lead); Methodology (equal); Project administration (equal); Writing - original draft (equal); Writing - review & editing (equal).
Jack J. Stallone: Investigation (supporting). **Megan Miaro:** Investigation (supporting). **Akshara Sharma:** Investigation (supporting). **Alan Grossfield:** Conceptualization (equal); Methodology (equal); Supervision (lead); Writing - review & editing (equal).

DATA AVAILABILITY

All analysis scripts, WESTPA configuration scripts, simulation snapshots, and source data are made available on GitHub (<https://github.com/Poruthoor/systemSizeEffectsInWEMD>) or upon request.

REFERENCES

- S. J. Singer and G. L. Nicolson, "The fluid mosaic model of the structure of cell membranes," *Science* **175**, 720–731 (1972).
- K. Simons and E. Ikonen, "Functional rafts in cell membranes," *Nature* **387**, 569–572 (1997).
- M. Edidin, "The state of lipid rafts: From model membranes to cells," *Annu. Rev. Biophys. Biomol. Struct.* **32**, 257–283 (2003).
- D. M. Engelman, "Membranes are more mosaic than fluid," *Nature* **438**, 578–580 (2005).
- E. Klotzsch and G. J. Schütz, "A critical survey of methods to detect plasma membrane rafts," *Philos. Trans. R. Soc., B* **368**, 20120033 (2013).
- S. L. Veatch and S. L. Keller, "Organization in lipid membranes containing cholesterol," *Phys. Rev. Lett.* **89**, 268101 (2002).
- S. L. Veatch and S. L. Keller, "Separation of liquid phases in giant vesicles of ternary mixtures of phospholipids and cholesterol," *Biophys. J.* **85**, 3074–3083 (2003).
- K. Simons and W. L. Vaz, "Model systems, lipid rafts, and cell membranes," *Annu. Rev. Biophys. Biomol. Struct.* **33**, 269–295 (2004).
- S. L. Veatch and S. L. Keller, "Seeing spots: Complex phase behavior in simple membranes," *Biochim. Biophys. Acta, Mol. Cell Res.* **1746**, 172–185 (2005).
- S. L. Veatch, S. S. W. Leung, R. E. W. Hancock, and J. L. Thewalt, "Fluorescent probes alter miscibility phase boundaries in ternary vesicles," *J. Phys. Chem. B* **111**, 502–504 (2007).
- S. Munro, "Lipid rafts," *Cell* **115**, 377–388 (2003).
- A. K. Kenworthy, "Have we become overly reliant on lipid rafts?," *EMBO Rep.* **9**, 531–535 (2008).
- E. Sezgin, I. Levental, S. Mayor, and C. Eggeling, "The mystery of membrane organization: Composition, regulation and roles of lipid rafts," *Nat. Rev. Mol. Cell Biol.* **18**, 361–374 (2017).
- I. Levental, K. R. Levental, and F. A. Heberle, "Lipid rafts: Controversies resolved, mysteries remain," *Trends Cell Biol.* **30**, 341–353 (2020).
- S. L. Veatch, N. Rogers, A. Decker, and S. A. Shelby, "The plasma membrane as an adaptable fluid mosaic," *Biochim. Biophys. Acta, Biomembr.* **1865**, 184114 (2023).
- S. A. Shelby, I. Castello-Serrano, K. C. Wissner, I. Levental, and S. L. Veatch, "Membrane phase separation drives responsive assembly of receptor signaling domains," *Nat. Chem. Biol.* **19**, 750–758 (2023).
- R. W. Pastor, R. M. Venable, and S. E. Feller, "Lipid bilayers, NMR relaxation, and computer simulations," *Acc. Chem. Res.* **35**, 438–446 (2002).

- ¹⁸S. J. Marrink, J. Risselada, and A. E. Mark, "Simulation of gel phase formation and melting in lipid bilayers using a coarse grained model," *Chem. Phys. Lipids* **135**, 223–244 (2005).
- ¹⁹J. D. Perlmutter and J. N. Sachs, "Interleaflet interaction and asymmetry in phase separated lipid bilayers: Molecular dynamics simulations," *J. Am. Chem. Soc.* **133**, 6563–6577 (2011).
- ²⁰W. D. Bennett and D. P. Tieleman, "Computer simulations of lipid membrane domains," *Biochim. Biophys. Acta, Biomembr.* **1828**, 1765–1776 (2013).
- ²¹A. J. Sodt, R. W. Pastor, and E. Lyman, "Hexagonal substructure and hydrogen bonding in liquid-ordered phases containing palmitoyl sphingomyelin," *Biophys. J.* **109**, 948–955 (2015).
- ²²D. S. Patel, S. Park, E. L. Wu, M. S. Yeom, G. Widmalm, J. B. Klauda, and W. Im, "Influence of ganglioside GM1 concentration on lipid clustering and membrane properties and curvature," *Biophys. J.* **111**, 1987–1999 (2016).
- ²³A. Bandara, A. Panahi, G. A. Pantelopulos, and J. E. Straub, "Exploring the structure and stability of cholesterol dimer formation in multicomponent lipid bilayers," *J. Comput. Chem.* **38**, 1479–1488 (2017).
- ²⁴S. A. Pandit, S. Vasudevan, S. Chiu, R. Jay Mashl, E. Jakobsson, and H. Scott, "Sphingomyelin-cholesterol domains in phospholipid membranes: Atomistic simulation," *Biophys. J.* **87**, 1092–1100 (2004).
- ²⁵G. Khelashvili, B. Kollmitzer, P. Heftberger, G. Pabst, and D. Harries, "Calculating the bending modulus for multicomponent lipid membranes in different thermodynamic phases," *J. Chem. Theory Comput.* **9**, 3866–3871 (2013).
- ²⁶A. J. Sodt, M. L. Sandar, K. Gawrisch, R. W. Pastor, and E. Lyman, "The molecular structure of the liquid-ordered phase of lipid bilayers," *J. Am. Chem. Soc.* **136**, 725–732 (2014).
- ²⁷M. Javanainen, H. Martinez-Seara, and I. Vattulainen, "Nanoscale membrane domain formation driven by cholesterol," *Sci. Rep.* **7**, 1143 (2017).
- ²⁸R.-X. X. Gu, S. Baoukina, D. P. Tieleman, and D. Peter Tieleman, "Phase separation in atomistic simulations of model membranes," *J. Am. Chem. Soc.* **142**, 2844–2856 (2020).
- ²⁹S. W. Canner, S. E. Feller, and S. R. Wassall, "Molecular organization of a raft-like domain in a polyunsaturated phospholipid bilayer: A supervised machine learning analysis of molecular dynamics simulations," *J. Phys. Chem. B* **125**, 13158–13167 (2021).
- ³⁰S. Dehghani-Ghahnaviyeh, M. Smith, Y. Xia, A. Dousis, A. Grossfield, and S. Sur, "Ionizable amino lipids distribution and effects on DSPC/cholesterol membranes: Implications for lipid nanoparticle structure," *J. Phys. Chem. B* **127**, 6928–6939 (2023).
- ³¹A. J. Poruthoor, A. Sharma, and A. Grossfield, "Understanding the free-energy landscape of phase separation in lipid bilayers using molecular dynamics," *Biophys. J.* **122**, 4144–4159 (2023).
- ³²G. A. Huber and S. Kim, "Weighted-ensemble Brownian dynamics simulations for protein association reactions," *Biophys. J.* **70**, 97–110 (1996).
- ³³B. W. Zhang, D. Jasnow, and D. M. Zuckerman, "The 'weighted ensemble' path sampling method is statistically exact for a broad class of stochastic processes and binning procedures," *J. Chem. Phys.* **132**, 054107 (2010).
- ³⁴D. M. Zuckerman and L. T. Chong, "Weighted ensemble simulation: Review of methodology, applications, and software," *Annu. Rev. Biophys.* **46**, 43–57 (2017).
- ³⁵J. Hénin, T. Lelièvre, M. R. Shirts, O. Valsson, and L. Delemotte, "Enhanced sampling methods for molecular dynamics simulations [article v1.0]," *Living J. Comput. Mol. Sci.* **4**, 1–60 (2022); [arXiv:2202.04164](https://arxiv.org/abs/2202.04164).
- ³⁶V. Privman, *Finite Size Scaling and Numerical Simulation of Statistical Systems* (World Scientific, 1990).
- ³⁷M. Mondello and G. S. Grest, "Viscosity calculations of *n*-alkanes by equilibrium molecular dynamics," *J. Chem. Phys.* **106**, 9327–9336 (1997).
- ³⁸M. Fushiki, "System size dependence of the diffusion coefficient in a simple liquid," *Phys. Rev. E* **68**, 021203 (2003).
- ³⁹I.-C. Yeh and G. Hummer, "System-size dependence of diffusion coefficients and viscosities from molecular dynamics simulations with periodic boundary conditions," *J. Phys. Chem. B* **108**, 15873–15879 (2004).
- ⁴⁰T. Iwashita, M. Nagao, A. Yoshimori, M. Terazima, and R. Akiyama, "Usefulness of higher-order system-size correction for macromolecule diffusion coefficients: A molecular dynamics study," *Chem. Phys. Lett.* **807**, 140096 (2022).
- ⁴¹V. Gapsys and B. L. de Groot, "On the importance of statistics in molecular simulations for thermodynamics, kinetics and simulation box size," *eLife* **9**, e57589 (2020).
- ⁴²M. N. Joswiak, N. Duff, M. F. Doherty, and B. Peters, "Size-dependent surface free energy and Tolman-corrected droplet nucleation of TIP4P/2005 water," *J. Phys. Chem. Lett.* **4**, 4267–4272 (2013).
- ⁴³J. B. Klauda, B. R. Brooks, A. D. MacKerell, R. M. Venable, and R. W. Pastor, "An *ab initio* study on the torsional surface of alkanes and its effect on molecular simulations of alkanes and a DPPC BILAYER," *J. Phys. Chem. B* **109**, 5300–5311 (2005).
- ⁴⁴J. B. Klauda, B. R. Brooks, and R. W. Pastor, "Dynamical motions of lipids and a finite size effect in simulations of bilayers," *J. Chem. Phys.* **125**, 144710 (2006).
- ⁴⁵M. Roark and S. E. Feller, "Molecular dynamics simulation study of correlated motions in phospholipid bilayer membranes," *J. Phys. Chem. B* **113**, 13229–13234 (2009).
- ⁴⁶B. A. Camley, M. G. Lerner, R. W. Pastor, and F. L. H. Brown, "Strong influence of periodic boundary conditions on lateral diffusion in lipid bilayer membranes," *J. Chem. Phys.* **143**, 243113 (2015).
- ⁴⁷J. J. Harris, G. A. Pantelopulos, and J. E. Straub, "Finite-size effects and optimal system sizes in simulations of surfactant micelle self-assembly," *J. Phys. Chem. B* **125**, 5068–5077 (2021).
- ⁴⁸Z. Jarin, O. Agolini, and R. W. Pastor, "Finite-size effects in simulations of peptide/lipid assembly," *J. Membr. Biol.* **255**, 437–449 (2022).
- ⁴⁹E. Braun, J. Gilmer, H. B. Mayes, D. L. Mobley, J. I. Monroe, S. Prasad, and D. M. Zuckerman, "Best practices for foundations in molecular simulations [article v1.0]," *Living J. Comput. Mol. Sci.* **1**, 1–28 (2019).
- ⁵⁰G. A. Pantelopulos, T. Nagai, A. Bandara, A. Panahi, and J. E. Straub, "Critical size dependence of domain formation observed in coarse-grained simulations of bilayers composed of ternary lipid mixtures," *J. Chem. Phys.* **147**, 095101 (2017).
- ⁵¹J. Huang and G. W. Feigenson, "Monte Carlo simulation of lipid mixtures: Finding phase separation," *Biophys. J.* **65**, 1788–1794 (1993).
- ⁵²Z. Zhang, M. Laradji, H. Guo, O. G. Mouritsen, and M. J. Zuckermann, "Phase behavior of pure lipid bilayers with mismatch interactions," *Phys. Rev. A* **45**, 7560–7567 (1992).
- ⁵³Y. Qi, H. I. Ingólfsson, X. Cheng, J. Lee, S. J. Marrink, and W. Im, "CHARMM-GUI martini maker for coarse-grained simulations with the martini force field," *J. Chem. Theory Comput.* **11**, 4486–4494 (2015).
- ⁵⁴S. J. Marrink, H. J. Risselada, S. Yefimov, D. P. Tieleman, and A. H. de Vries, "The MARTINI force field: Coarse grained model for biomolecular simulations," *J. Phys. Chem. B* **111**, 7812–7824 (2007).
- ⁵⁵D. H. de Jong, G. Singh, W. F. D. Bennett, C. Arnarez, T. A. Wassenaar, L. V. Schäfer, X. Periole, D. P. Tieleman, and S. J. Marrink, "Improved parameters for the martini coarse-grained protein force field," *J. Chem. Theory Comput.* **9**, 687–697 (2013).
- ⁵⁶S. O. Yesylevsky, L. V. Schäfer, D. Sengupta, and S. J. Marrink, "Polarizable water model for the coarse-grained MARTINI force field," *PLoS Comput. Biol.* **6**, e1000810 (2010).
- ⁵⁷M. J. Abraham, T. Murtola, R. Schulz, S. Páll, J. C. Smith, B. Hess, E. Lindahl, and E. Lindahl, "GROMACS: High performance molecular simulations through multi-level parallelism from laptops to supercomputers," *SoftwareX* **1–2**, 19–25 (2015).
- ⁵⁸H. I. Ingólfsson, M. N. Melo, F. J. van Eerden, C. Arnarez, C. A. Lopez, T. A. Wassenaar, X. Periole, A. H. de Vries, D. P. Tieleman, and S. J. Marrink, "Lipid organization of the plasma membrane," *J. Am. Chem. Soc.* **136**, 14554–14559 (2014).
- ⁵⁹X. Lin and A. A. Gofre, "Understanding membrane domain-partitioning thermodynamics of transmembrane domains with potential of mean force calculations," *J. Phys. Chem. B* **123**, 1009–1016 (2019).
- ⁶⁰J. Su, S. J. Marrink, M. N. Melo, and A. M. Grossfield, "Localization preference of antimicrobial peptides on liquid-disordered membrane domains," *Front. Cell Dev. Biol.* **8**, 1–11 (2020).
- ⁶¹M. Abraham, A. Alekseenko, C. Bergh, C. Blau, E. Briand, M. Doijade, S. Fleischmann, V. Gapsys, G. Garg, S. Gorelov, G. Gouaillardet, A. Gray, M. E. Irrgang, F. Jalalypour, J. Jordan, C. Junghans, P. Kanduri, S. Keller, C. Kutzner, J. A. Lemkul, M. Lundborg, P. Merz, V. Miletic, D. Morozov, S. Páll, R. Schulz, M. Shirts, A. Shvetsov, B. Soproni, D. van der Spoel, P. Turner, C. Uphoff, A. Villa,

- S. Wingbermühle, A. Zhmurov, P. Bauer, B. Hess, and E. Lindahl, GROMACS 2023 Manual, 2023.
- ⁶²D. H. de Jong, S. Baoukina, H. I. Ingólfsson, and S. J. Marrink, “Martini straight: Boosting performance using a shorter cutoff and GPUs,” *Comput. Phys. Commun.* **199**, 1–7 (2016).
- ⁶³W. F. Van Gunsteren, H. J. Berendsen, and J. A. Rullmann, “Inclusion of reaction fields in molecular dynamics: Application to liquid water,” *Faraday Discuss. Chem. Soc.* **66**, 58–70 (1978).
- ⁶⁴L. Verlet, “Computer ‘experiments’ on classical fluids. I. Thermodynamical properties of Lennard-Jones molecules,” *Phys. Rev.* **159**, 98–103 (1967).
- ⁶⁵M. Parrinello and A. Rahman, “Polymorphic transitions in single crystals: A new molecular dynamics method,” *J. Appl. Phys.* **52**, 7182–7190 (1981).
- ⁶⁶G. Bussi, D. Donadio, and M. Parrinello, “Canonical sampling through velocity rescaling,” *J. Chem. Phys.* **126**, 14101 (2007); [arXiv:0803.4060](https://arxiv.org/abs/0803.4060).
- ⁶⁷B. Hess, H. Bekker, H. J. C. Berendsen, and J. G. E. M. Fraaije, “LINCS: A linear constraint solver for molecular simulations,” *J. Comput. Chem.* **18**, 1463–1472 (1997).
- ⁶⁸S. Thallmair, M. Javanainen, B. Fábán, H. Martínez-Seara, and S. J. Marrink, “Nonconverged constraints cause artificial temperature gradients in lipid bilayer simulations,” *J. Phys. Chem. B* **125**, 9537–9546 (2021).
- ⁶⁹G. Fiorin, M. L. Klein, and J. Hénin, “Using collective variables to drive molecular dynamics simulations,” *Mol. Phys.* **111**, 3345–3362 (2013).
- ⁷⁰X. X. Martin Ester, H.-P. Kriegel, and J. Sander, “A density-based algorithm for discovering clusters in large spatial databases with noise,” in *Proceedings of the 2nd ACM International Conference on Knowledge Discovery and Data Mining (KDD)* (AAAI Press, 1996), pp. 226–231.
- ⁷¹E. Schubert, J. Sander, M. Ester, H. P. Kriegel, and X. Xu, “DBSCAN revisited, revisited,” *ACM Trans. Database Syst.* **42**, 1–21 (2017).
- ⁷²E. Pedregosa, F. Varoquaux, G. Gramfort, A. Michel, V. Thirion, B. Grisel, O. Blondel, M. Prettenhofer, P. Weiss, R. and Dubourg, V. Vanderplas, J. Passos, A. Cournapeau, D. Brucher, M. Perrot, and M. Duchesnay, “Scikit-learn: Machine learning in python,” *J. Mach. Learn. Res.* **12**, 2825–2830 (2011).
- ⁷³A. T. Bogetti, J. M. G. Leung, J. D. Russo, S. Zhang, J. P. Thompson, A. S. Saglam, D. Ray, R. C. Abraham, J. R. Faeder, I. Andricioaei, J. L. Adelman, M. C. Zwier, D. N. LeBard, D. M. Zuckerman, and L. T. Chong, “A suite of advanced tutorials for the WESTPA 2.0 rare-events sampling software [article v2.0],” *Living J. Comput. Mol. Sci.* **5**, 1655 (2022).
- ⁷⁴J. D. Russo, S. Zhang, J. M. G. Leung, A. T. Bogetti, J. P. Thompson, A. J. DeGrave, P. A. Torrillo, A. J. Pratt, K. F. Wong, J. Xia, J. Copperman, J. L. Adelman, M. C. Zwier, D. N. LeBard, D. M. Zuckerman, and L. T. Chong, “WESTPA 2.0: High-performance upgrades for weighted ensemble simulations and analysis of longer-timescale applications,” *J. Chem. Theory Comput.* **18**, 638–649 (2022).
- ⁷⁵A. T. Bogetti, B. Mostofian, A. Dickson, A. J. Pratt, A. S. Saglam, P. O. Harrison, J. L. L. Adelman, M. Dudek, P. A. Torrillo, A. J. DeGrave, U. Adhikari, M. C. Zwier, D. M. Zuckerman, and L. T. Chong, “A suite of tutorials for the WESTPA rare-events sampling software [article v1.0],” *Living J. Comput. Mol. Sci.* **1**, 1–32 (2019).
- ⁷⁶P. A. Torrillo, A. T. Bogetti, and L. T. Chong, “A minimal, adaptive binning scheme for weighted ensemble simulations,” *J. Phys. Chem. A* **125**, 1642–1649 (2021).
- ⁷⁷D. Bhatt, B. W. Zhang, and D. M. Zuckerman, “Steady-state simulations using weighted ensemble path sampling,” *J. Chem. Phys.* **133**, 014110 (2010).
- ⁷⁸E. Suárez, S. Lettieri, M. C. Zwier, C. A. Stringer, S. R. Subramanian, L. T. Chong, and D. M. Zuckerman, “Simultaneous computation of dynamical and equilibrium information using a weighted ensemble of trajectories,” *J. Chem. Theory Comput.* **10**, 2658–2667 (2014); [arXiv:1210.3094](https://arxiv.org/abs/1210.3094).
- ⁷⁹T. D. Romo, N. Leioatts, and A. Grossfield, “Lightweight object oriented structure analysis: Tools for building tools to analyze molecular dynamics simulations,” *J. Comput. Chem.* **35**, 2305–2318 (2014).